Chapter

3

Preparation, Characterization, and Physical Properties of Deep Eutectic Solvents

Contents

3.1 Introduction

3.2 Experimental section

3.3 Result and discussion

3.3.1 Preparation and characterization DESs

a) Preparation and characterization of type-III DESs (reline, ethaline, and glyceline)

b) Preparation and characterization of water-based DESs (aquolines)

c) Preparation and characterization of type-V DESs (hydrophobic DESs; HDES)

d) Preparation and characterization of ternary DESs (TDESs)

3.3.2 Physical properties of prepared DESs and DES-water mixture

3.4 Conclusion

3.5 References

This chapter describes the preparation, characterization, and physical properties of various types of deep eutectic solvents (DESs) including type-III DESs, ternary DESs, water-based DESs, and hydrophobic DESs.

3.1. Introduction

The synthesis and purification of ionic liquids (ILs) and molecular solvents involve complex and multiple steps [1]. Due to the complexity of these synthesis and purification processes, ILs are expensive and difficult to prepare [2]. On the other hand, deep eutectic solvents (DESs) can be prepared by simply mixing and heating each of their components in a eutectic ratio, or by dissolving each component in an appropriate solvent and then letting the solvent evaporate [3]. DESs can be efficiently produced by using cost-effective quaternary ammonium (choline chloride, ChCl), phosphonium, or sulfonium cation salts (hydrogen bond acceptor, HBA) and hydrogen bond donors (HBDs) through easy synthesis methods and without any further purification which reduces the overall cost of these solvents [1,3].

The initial development or combination of a quaternary ammonium salt with a HBD was conducted by Abbot et al. in 2002 [4]. Abbot discovered that a molar ratio of choline chloride to urea of 1:2 gives a eutectic solvent with a melting point of 12 ºC. DESs are formed through the combination of appropriate HBDs and HBAs in eutectic ratio, without involving any chemical processes. Consequently, it is more accurate to describe this procedure as "preparation" rather than "synthesis" [5]. Numerous methods have been employed in the literature for the preparation of DES, including the use of a mortar and pestle to combine the components (griding) [5], stirring the components while gently heating them to make a homogenous mixture [6,7], freeze-drying [8], ball milling [9], microwave radiation [10,11], and rotary evaporation [12,13]. **Scheme 3.1** gives various methods for the preparation of DES.

The thermal or heat-treatment method (heating and stirring approach) has been widely employed as the predominant methodology for the preparation of DESs since the beginning. Thermal treatment is frequently utilized in the process of formulating DESs with melting points lower than 80 ºC [1]. The development of the DES complex is dependent on the DES components, the temperature at which the heating is done, the amount of time that the heating is done, and/or stirring. The temperature is precisely determined by considering the melting point, boiling point, and stability of constituents. The heating process is typically done within the temperature range of 60 to 80 ºC, with a gentle stirring in order to prevent the disruption of

the hydrogen bonds that have been formed. In addition, non-thermal techniques have been employed for the preparation of DESs. These methods of preparation frequently involve the use of agitation at elevated velocities. These procedures are most effectively employed in the synthesis or formulation of DESs that possess melting points equal to or lower than the ambient temperature [14]. Nonthermal techniques involve several processes such as sonication, vortex mixing, and freeze-drying [15].

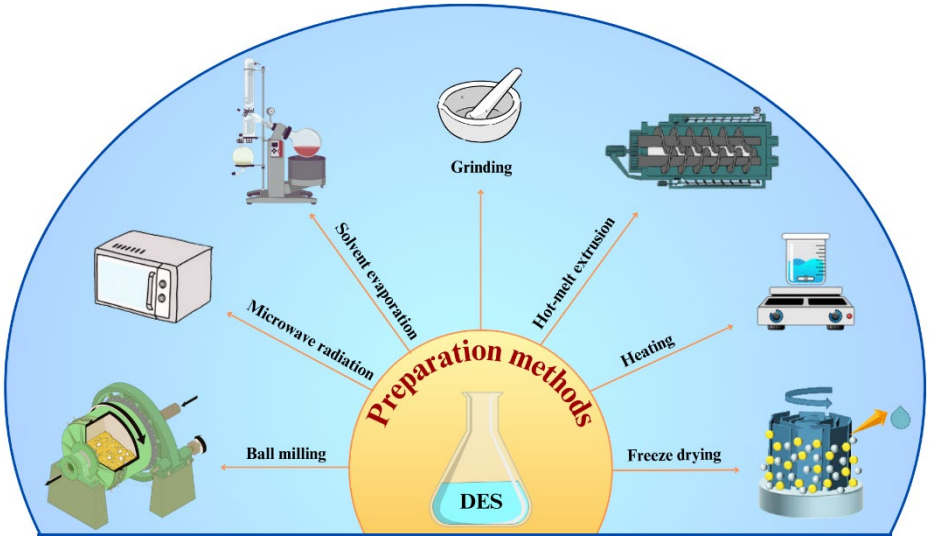

Scheme 3.1: Preparation methods for DESs [16].

To evaluate the potential of DESs as alternative solvents, to replace traditional molecular solvents and ILs in diverse applications, it is essential to have a comprehensive understanding of their physical, chemical, and thermal characteristics. The application of newly developed compounds depends on their thermal and physicochemical characteristics [17–19]. The state of a compound is influenced by many thermal and physicochemical characteristics. Therefore, understanding these characteristics influences the selection and approach to implementation. For example, understanding viscosity can aid in the suitable choice of a solvent and temperature appropriate for a specific application, thereby resulting in material and energy conservation [20]. These physicochemical and thermal characteristics include density, conductivity, pH, refractive index, viscosity, and surface tension.

The concept of pH is used to characterize the acidic or basic nature of the material. The solvent characteristic in concern has significant importance as it exerts influence on extractions, reactions, and design factors related to corrosion. The acidity or basicity of a solvent affects its reactivity and effectiveness as a reaction medium [21,22]. The determination of density is an essential factor in the development of chemical materials and the design of processes that include fluid mechanics and mass transfer calculations [23,24]. The density of a solvent

influences its mass flow and thus determines its suitability for various chemical processes or separations. Surface tension is a fundamental characteristic that measures the cohesive forces present at the interface of a liquid [25]. By determining this property, it can acquire insights into the inherent energy interactions between molecules within the liquid. This physical attribute holds significant importance in various practical contexts, including the assessment of wettability, the efficiency of mass transfer in liquid-liquid or gas-liquid extraction processes, and its relevance in multi-phasic homogeneous catalysis [26–28].

In the present study, various varieties of DESs are produced through the modification of components and their molar ratios in order to investigate the association behaviour of surfactants within them. The synthesized DESs were subjected to characterization using ^{1}H NMR and IR spectroscopic techniques. The physicochemical parameters of the synthetic DES and the mixture of reline and water have been determined. These properties include zero shear viscosity, relative viscosity, surface tension, conductivity, density, and refractive index. Among the synthesized DESs, some of them are ternary while the others are binary. It is important to highlight that there is a limited amount of research documented in the existing literature regarding ternary eutectic systems [29–31].

3.2 Experimental section

The materials and methods used are discussed in chapter 2.

3.3 Result and discussion

3.3.1 Preparation and characterization DESs

The DESs used in this study were synthesized and characterized using procedures described in the literature [32,33].

3.3.1.1 Preparation of various DESs

a) Preparation of type-III DESs (reline, ethaline, and glyceline)

Reline was synthesized and characterized using a similar process as previously documented [34,35]. In general, dehydrated ChCl and urea were combined in a 1:2 molar ratio and subjected to heating at 353 K for about 2 h while being continuously stirred until a transparent liquid was formed. The fluid was subjected to a 24 h equilibration process at 313 K in a vacuum oven. The schematic representation of the process and possible interactions in reline is represented in **Scheme 3.2.**

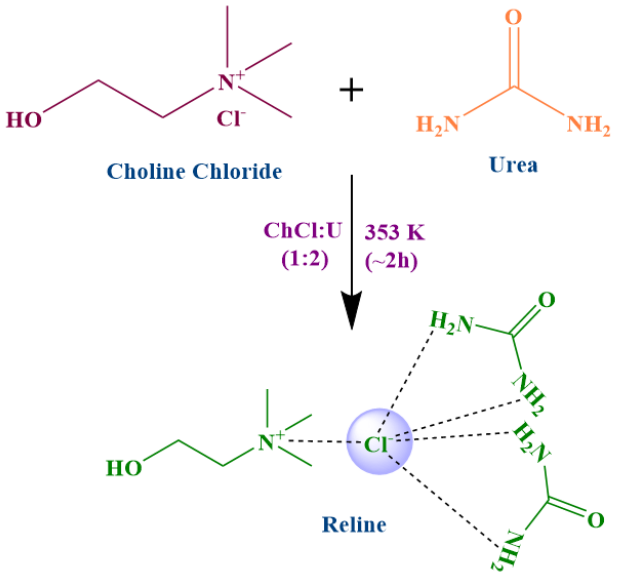

Scheme 3.2: Preparation of reline.

Ethaline is a DES composed of a single mole of choline chloride and two moles of ethylene glycol and it was prepared by adopting a previously reported procedure [36]. The appropriate proportions of dehydrated choline chloride and ethylene glycol were measured using a highly accurate digital balance and placed in a sealed bottle. A bottle is subjected to heating at 333 K for about 2 h with continuous stirring. After the formation of a homogenous mixture, the vial was transferred to a vacuum oven and subjected to a temperature of 313 K for 24 h to evaporate any moisture present in the prepared Ethaline. The schematic representation of the process and possible interactions in ethaline is represented in **Scheme 3.3.**

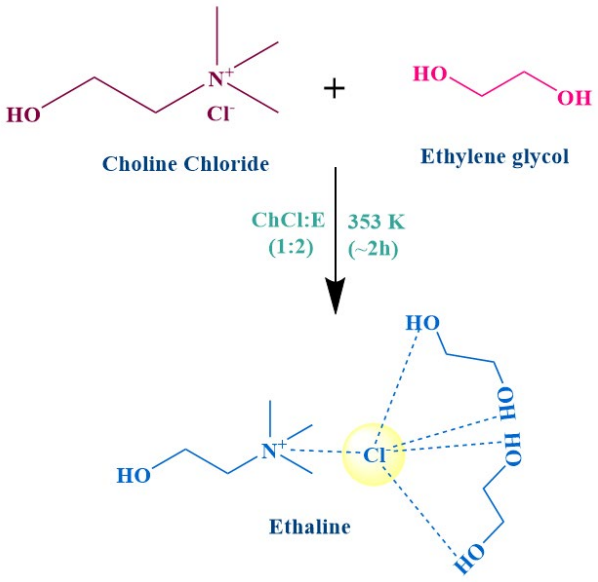

Scheme 3.3: Preparation of ethaline

Glyceline was synthesized and characterized using a similar process as previously documented [1]. Dehydrated ChCl and glycerol were mixed in a 1:2 molar ratio and were subjected to heating at 353 K for about 2 h with continuously stirred until a homogenous liquid was formed. The fluid was subjected to a 24 h equilibration process at 313 K in a vacuum oven. The schematic representation of the process and possible interactions in glyceline is represented in **Scheme 3.4.**

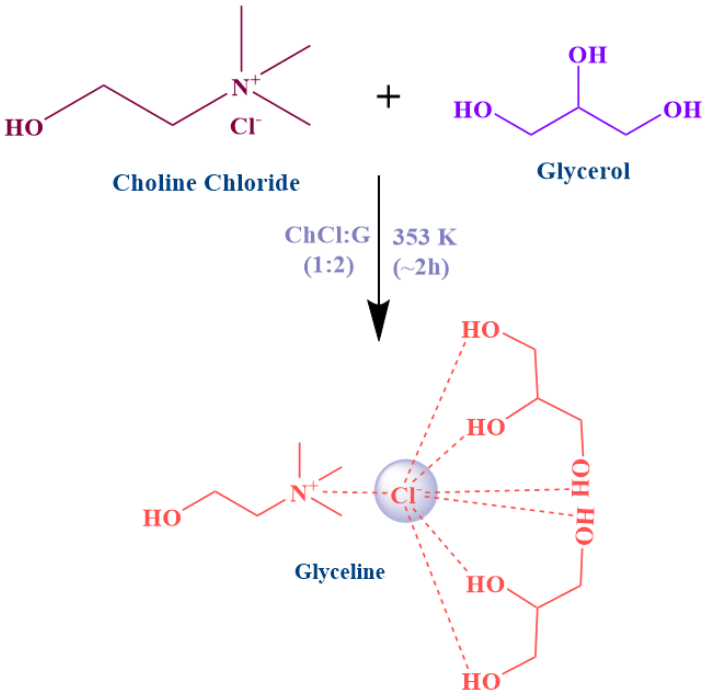

Scheme 3.4: Preparation of glyceline

b) Preparation of water-based DESs (aquolines)

Aquoline was formed by following a reported procedure [37] in which anhydrous choline chloride and water were mixed in ratios of 1:2 (DES I), 1:3 (DES II), 1:4 (DES III), and 1:5 (DES IV). The mixture was placed in a closed bottle and stirred continuously at 600 rpm for 30 minutes at ambient temperature and pressure until a uniform liquid was formed. The solvents were observed for one hour to verify the presence of any residual crystals in the base of the bottle. Obtained transparent homogenous fluid was equilibrated for 1 h in a paraffin-sealed bottle and was later stored in a desiccator. The schematic representation of the process and possible interactions in aquolines is represented in **Scheme 3.5**.

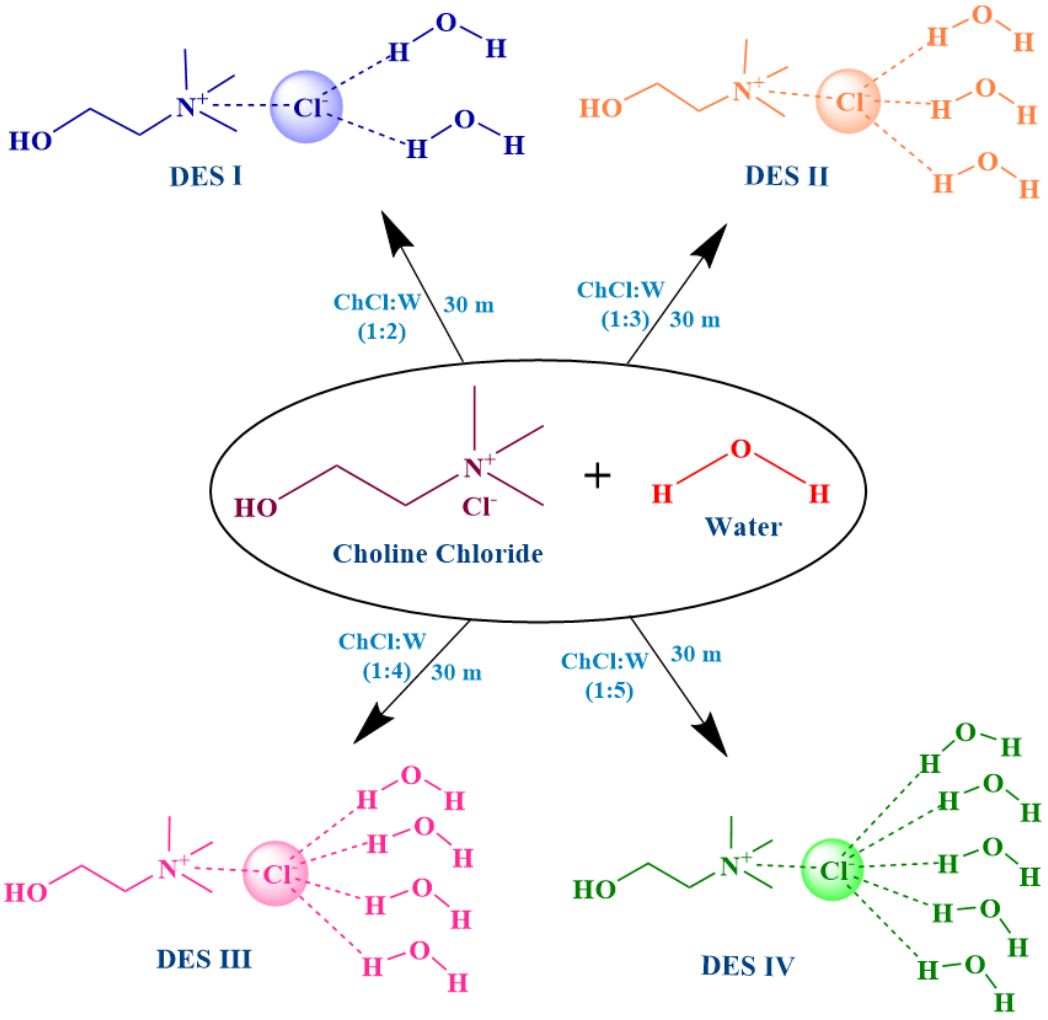

Scheme 3.5: Preparation of aquolines.

c) Preparation of type-V DESs (hydrophobic DESs; HDES)

Hydrophobic DESs were synthesized using a similar process as previously reported [38,39]. The preparation of HDES involved the mixing of eutectic-forming components (camphor, menthol, and thymol) in eutectic ratios (T: M-1:1; TM11, T: M-1:2; TM12, T: M-2:1; TM21, C: T: M-1:1:1; CTM111) using a magnetic stirrer. A precisely measured quantity of eutectic-forming components was placed in a screw-capped glass bottle. Afterward, the glass bottle was subjected to heating at 308-313 K (if needed) for about 1 h with continuous stirring until a homogenous liquid was formed. The schematic representation of the process and possible interactions in HDES is represented in **Scheme 3.6**.

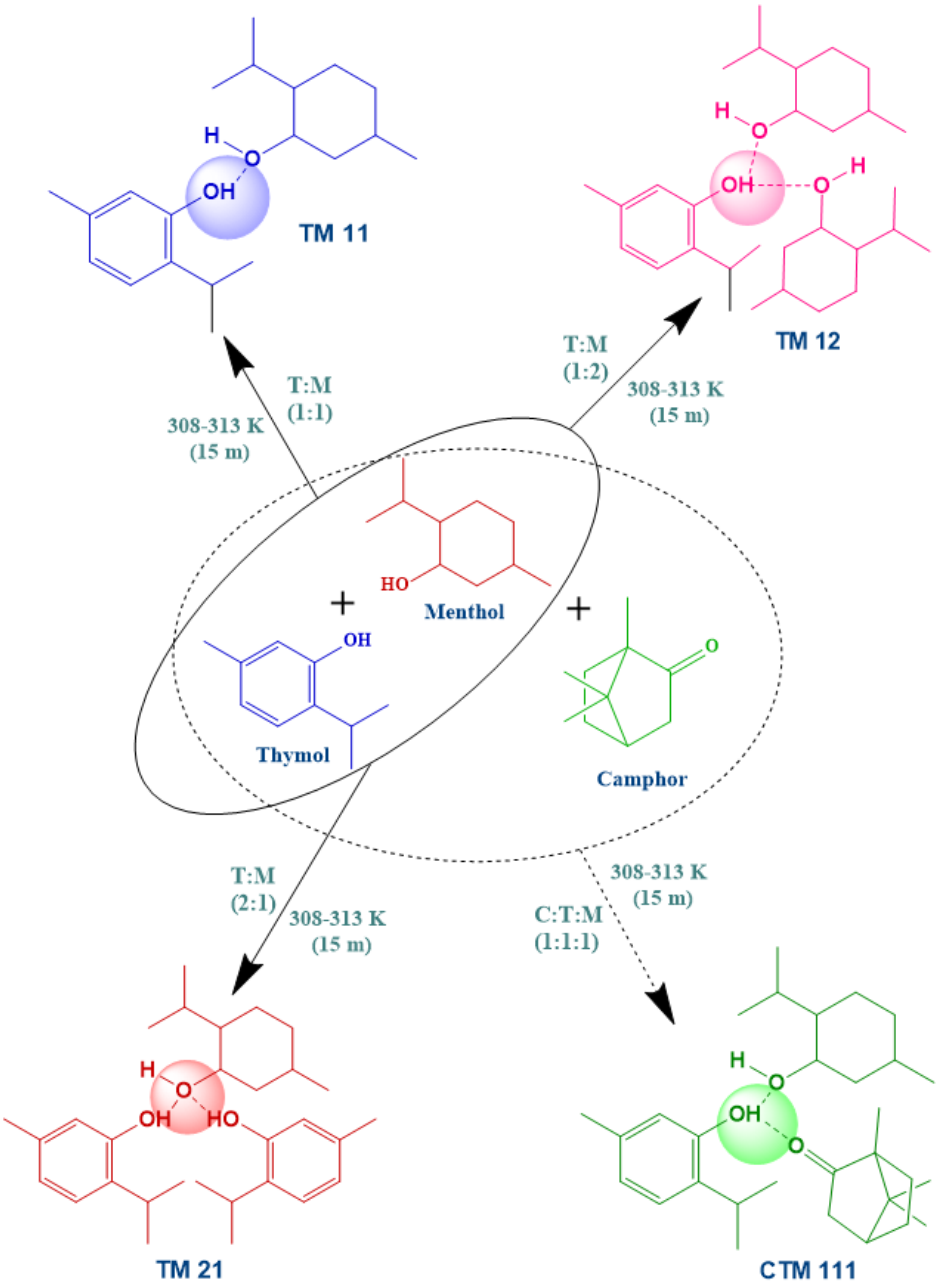

Scheme 3.6: Preparation of hydrophobic DESs.

d) Preparation of ternary DESs (TDESs)

The TDES samples were produced using varying molar ratios of ChCl: urea: glycerol, specifically 1:1:1 (CUG I), and 1:1.5:0.5 (CUG II). TDES combinations were synthesized at ambient pressure by combining previously dried ChCl, urea, and glycerol at a temperature of 333 K, using various molar ratios. The mixtures were agitated while being heated until uniform colorless liquids were produced. The TDES samples were subjected to vacuum drying at a temperature of 313 K overnight to remove any moisture before characterizations [40,41]. The schematic representation of the process is represented in **Scheme 3.7**.

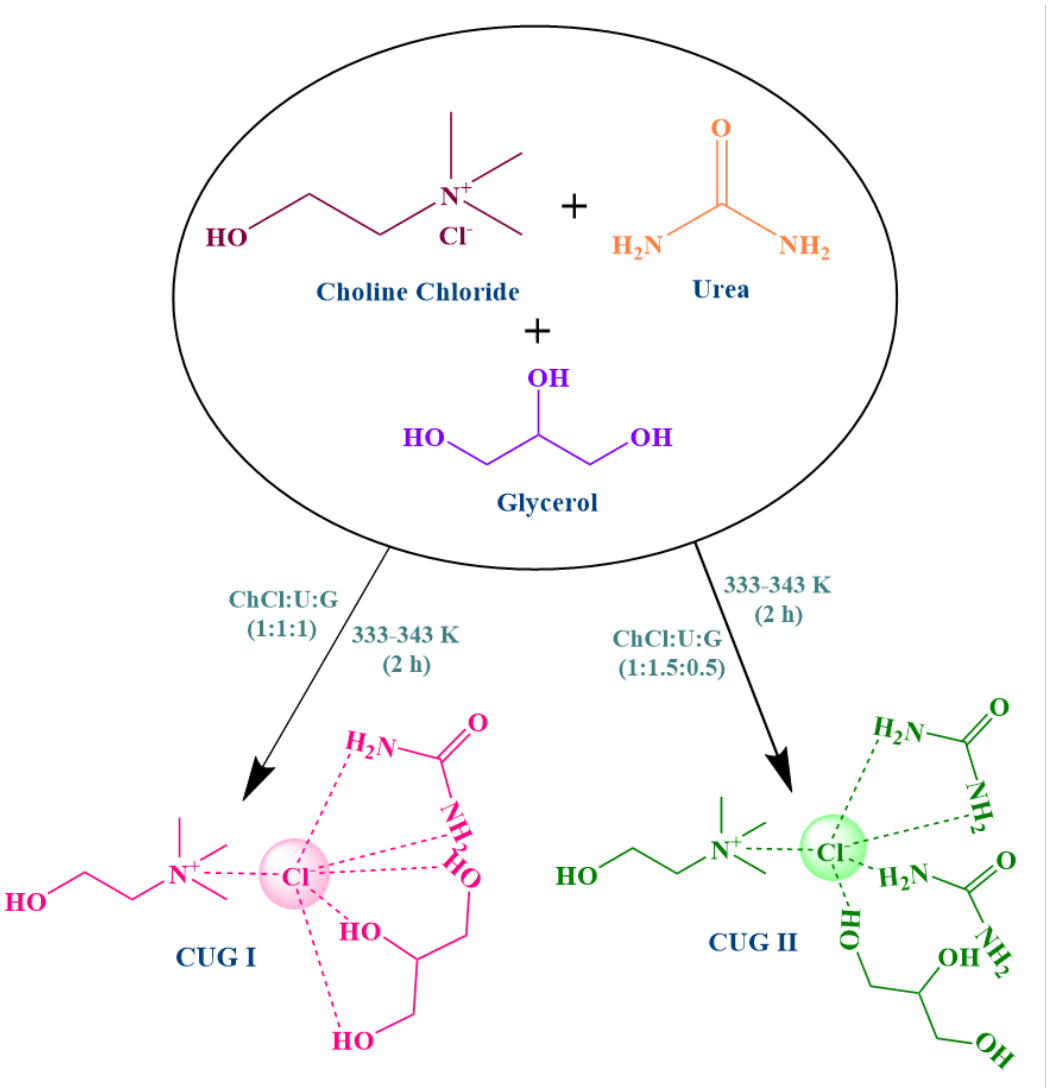

Scheme 3.7: Preparation of ternary DESs (TDESs)

All DES samples were synthesized at atmospheric pressure and under tight control of moisture content and were kept in airtight vials for storage in a moisture-controlled desiccator.

3.3.1.2 Characterization of prepared DESs

All the prepared DESs were characterized by FTIR and ^{1}H-NMR using a similar process as previously documented [42–44]. The characterization data was also compared with previous studies.

a) Characterization of type-III DESs (reline, ethaline, and glyceline)

The initial characterization of reline, ethaline, and glyceline along with its starting components was conducted using FTIR spectroscopy, and the resulting spectrum is depicted in **Figure 3.1 (a-c).**

The FTIR spectroscopy of ChCl, urea, and reline is represented in **Figure 3.1 (a)**. The IR spectrum of reline is a mixture of frequencies from the IR spectra of ChCl and urea, with minor frequency changes. The frequencies at 3258 cm^{-1} in ChCl are attributed to the -CH_3 stretching vibrations. The frequencies at 3442 cm^{-1} and 3340 cm^{-1} in Urea correspond to the coupled vibrations of –NH_2 symmetric vibration of stretching and antisymmetric stretching vibration, correspondingly. The band at 3235 cm^{-1} is associated with bending vibrations of the –NH_2 group. The ranges of frequencies at 1684 cm^{-1} and 1603 cm^{-1} are the distinctive vibration frequencies of –$CONH_2$. In reline, the bands move to a lower frequency and become broader. The observation shows the development of hydrogen bonds among ChCl and Urea. Hydrogen bonds decrease the force constants of the initial bonds, leading to a decrease and widening of its absorption frequency. The system can have hydrogen bonds in the form of –NH-OH–, –NH-NH–, –OH-OH–, –OH-NH–. The IR spectrum indicates the existence of hydrogen bonding, which accounts for the existence of reline in a liquid state at ambient temperature.

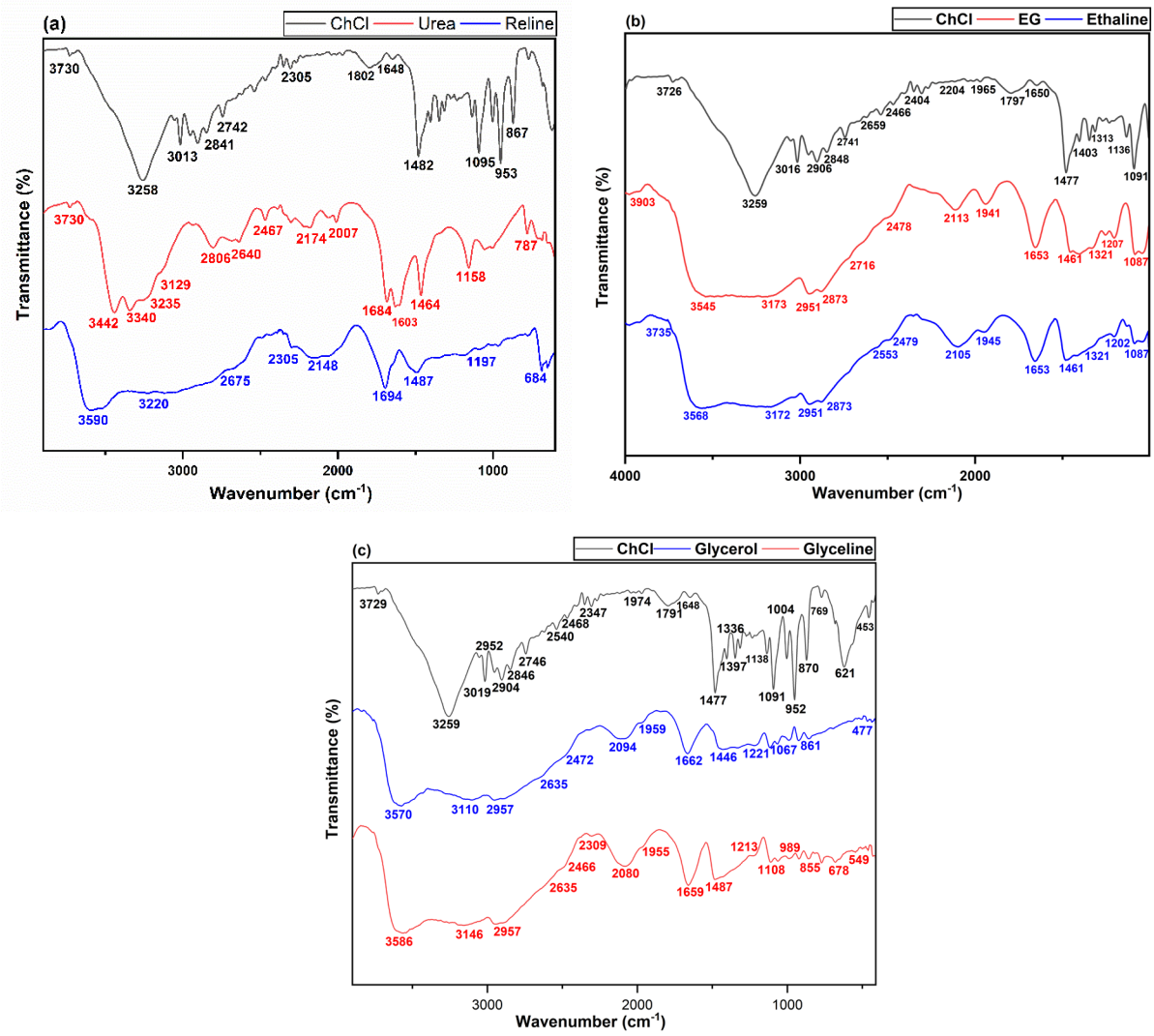

Figure 3.1: FTIR spectra of a) reline b) ethaline and c) glyceline.

Ethaline has a broad and intense band, characteristic of intramolecular –OH bonds, suggesting the development of additional hydrogen bonds at 3568-3569 cm^{-1}. The production of new hydrogen bonds is significantly characterized by an absorption band at 3172 cm^{-1}, peculiar to OH-NH or NH-O type bonds, which is also associated with the vibration band at 1653 cm^{-1}. Bands specific to the CCO- group could be seen at 1087 cm^{-1} (**Figure 3.1 (b)**).

Figure 3.1 (c) displays peaks in the range of 3570-3110 cm^{-1} in glycerol, which can be attributed to the stretching vibration of the O−H functional group. The peaks at 3146 cm^{-1} in the glyceline indicate the stretching vibration of the O− H functional group following the creation of the glyceline. The N−H stretching of ChCl overlaps with the O−H stretching between 3110 and 3259 cm^{-1}. **Figure 3.1 (c)** shows that the FTIR absorption peaks of glycerol's O−H functional group shift to lower wavenumbers and exhibit a noticeable red shift after forming glyceline. This indicates that the O−H functional group of glycerol takes part in the formation of hydrogen bonding interactions among ChCl anions. The degree of red-shifting in FTIR absorption peaks of the O−H functional group of glycerol as a hydrogen bond donor is inconsistent, suggesting that the strength of hydrogen bonding contact between ChCl and the O−H functional group of the hydrogen bond donor is different.

The DESs (reline, ethaline, and glyceline) were subjected to further characterization using ^{1}H-NMR spectroscopy, as depicted in **Figure 3.2.** Signals (δ ppm) are observed corresponding with the literature data [44–46]. **Figure 3.2 (a)** displays the ^{1}H NMR spectra of reline. The wide line widths seen in the ^{1}H NMR spectrum of reline suggest that reline has a higher viscosity. The signals for different interactions for reline are shown as: ^{1}H NMR (400 MHz, DMSO) δ 5.57 (t, J = 4.8 Hz, 8H), 3.91 – 3.74 (m, 2H), 3.47 – 3.41 (m, 2H), 3.14 (s, 9H).

Figure 3.2 (b) displays the ^{1}H NMR spectrum of ethaline. The small broadening of the peaks at the bottom is primarily caused by the characteristics of the samples. Consequently, inter and intra-dipolar interactions are likely to induce a broadening effect on the NMR spectrum's line shapes. The signals for different interactions for ethaline are shown as: ^{1}H NMR (400 MHz, DMSO) δ 5.54 (t, J = 5.1 Hz, 1H), 4.55 (t, J = 5.3 Hz, 4H), 3.87 – 3.80 (m, 2H), 3.47 – 3.33 (m, 11H), 3.16 (d, J = 19.4 Hz, 9H).

Figure 3.2 (c) displays the ^{1}H NMR spectra for the glyceline. In the glyceline, the characteristic signals of both ChCl and glycerol protons were shifted to higher frequencies compared to when they were in separate solutions in D_2O. The downfield chemical changes

are a result of the ion−hydrogen bond donor complex development that defines the formation of glyceline. The signals for different interactions for glyceline are shown as: ^{1}H NMR (400 MHz, DMSO) δ 5.49 (t, J = 5.1 Hz, 1H), 4.57 (t, J = 9.4 Hz, 2H), 4.61 – 4.46 (m, 4H), 3.87 – 3.76 (m, 2H), 3.52 – 3.40 (m, 4H), 3.31 (ddt, J = 21.7, 10.9, 5.4 Hz, 8H), 3.14 (s, 9H).

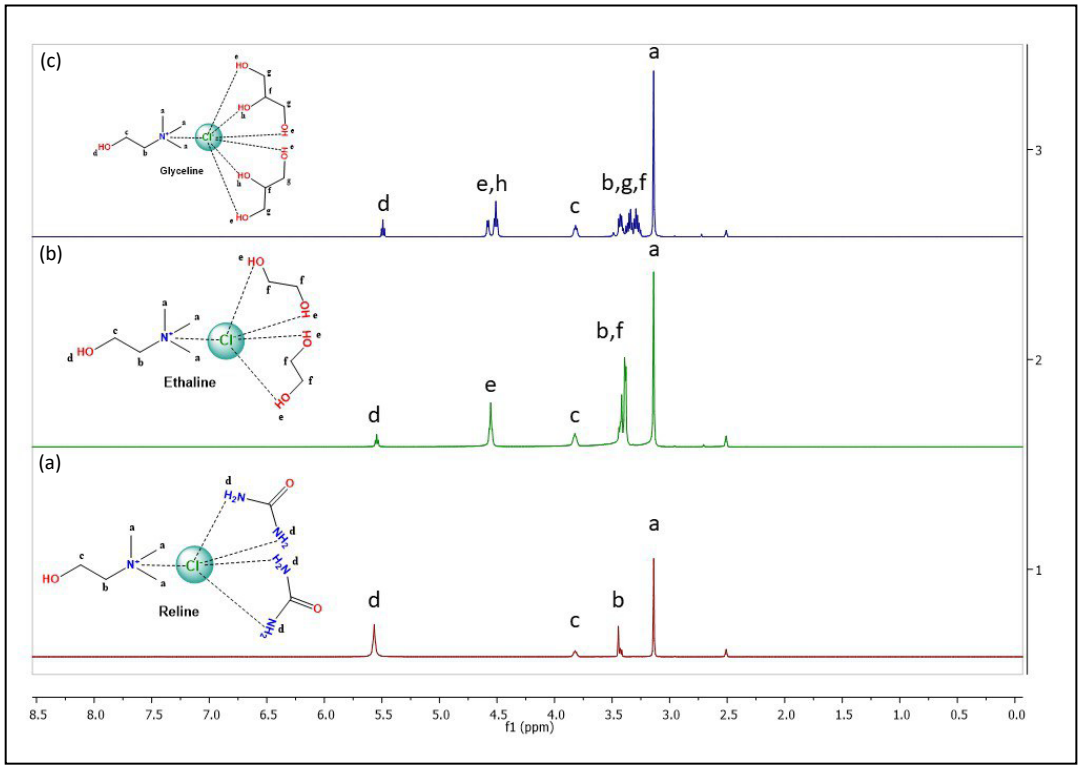

Figure 3.2: ^{1}H-NMR spectra of a) reline b) ethaline and c) glyceline.

b) Characterization of water-based DESs (aquolines)

Figures 3.3 and 3.4 show typical FTIR and NMR spectra for various aquolines, respectively. DES I to IV are formed by mixing ChCl with different molar ratios of water as mentioned earlier. **Figure 3.3** shows FTIR spectra of pure ChCl and various synthesized aquolines (DES I to DES IV). The presence of water molecules in the network of ChCl (in a typical DES) leads to distinct changes in the frequency shift in the IR bands owing to hydrogen bonding interactions. In pure ChCl, the -OH peak (at 3020 cm^{-1}) gradually broadens as water molecules increase with a concomitant indication of hydrogen bonding. A similar type of peak broadening has been observed in a well-known DES (reline) on the addition of water and corroborates present results [42]. Another feature of IR spectra is the peak broadening at 1646 cm^{-1} which is indicative of interaction between water molecules and ChCl. However, in DES IV (with the highest water molecules, ChCl: H_2O, 1:5) the peak broadening is checked (3020 cm^{-1}) and matched with the IR spectrum of pure ChCl. This is an indication of the gradual

transition of DESs (with higher water molecules) into a molecular solution of ChCl in water. This has been further confirmed by other physicochemical measurements.

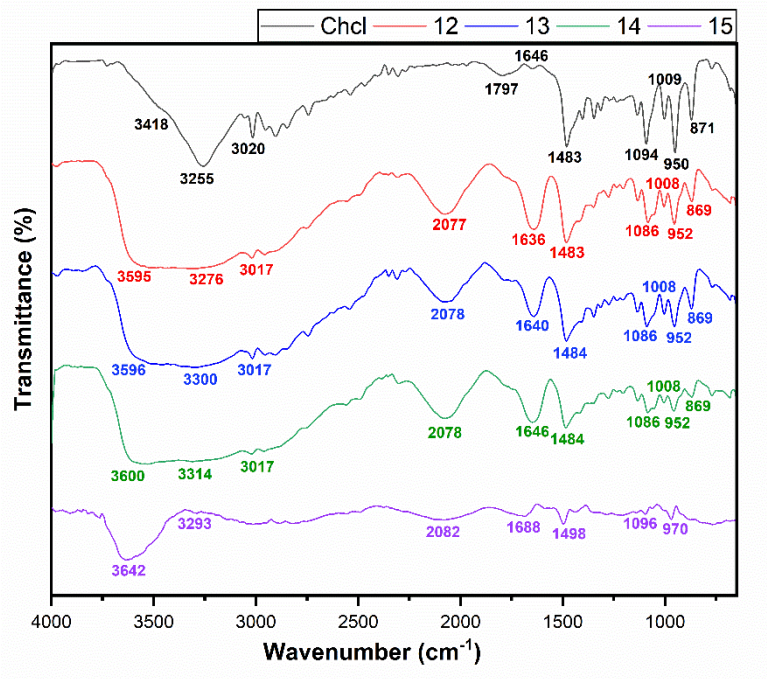

Figure 3.3: FTIR spectra of aquolines.

The synthesized aquolines were further characterized by ^{1}H NMR. **Figure 3.4** shows the ^{1}H NMR of ChCl: H_2O (aquoline) with a ratio of 1:2 (DES I), 1:3 (DES II), 1:4 (DES III), and 1:5 (DES IV) from the bottom. As hydrogen bonding increases, the ^{1}H NMR signal shows displacement toward the downfield. The relative comparison of peak intensity leads to information regarding the number of hydrogen molecules that take part in hydrogen bonding. The signals for different interactions for DES I are shown as: ^{1}H NMR (400 MHz, DMSO) δ 5.68 (t, J = 5.2 Hz, 1H), 3.81 (s, 2H), 3.52 (s, 4H), 3.49 – 3.42 (m, 2H), 3.16 (s, 9H), for DES II: ^{1}H NMR (400 MHz, DMSO) δ 5.64 (t, J = 5.2 Hz, 1H), 3.85 – 3.76 (m, 2H), 3.51 (s, 6H), 3.47 – 3.41 (m, 2H), 3.15 (s, 9H), for DES III: ^{1}H NMR (400 MHz, DMSO) δ 5.62 (t, J = 5.2 Hz, 1H), 3.92 – 3.72 (m, 2H), 3.48 (s, 8H), 3.44 (d, J = 5.2 Hz, 2H), 3.15 (s, 9H), and for DES IV: ^{1}H NMR (400 MHz, DMSO) δ 5.59 (t, J = 5.1 Hz, 1H), 3.80 (d, J = 4.6 Hz, 2H), 3.74 (s, 10H), 3.48 – 3.41 (m, 2H), 3.14 (s, 9H).

Choline chloride contains one quaternary nitrogen that is attached to a chloride ion and that chloride ion works as a junction between cholinium ion (Ch^+) and H_2O molecules (due to H-bonding(s)) that show the overall effect on chemical shift (δ) of trimethyl group bounded to quaternary nitrogen on moving from DES I to DES III. A small variation in δ was observed (3.16 ppm to 3.14 ppm) for 9 hydrogens that belong to the trimethyl group attached to

quaternary nitrogen. However, the side peak belongs to the water proton observed in the range of 3.48-3.52 ppm for 4H, 6H, and 8H for DES I to DES III, respectively. This implies that for DES I, each choline chloride has internal interaction with two water molecules, for DES II with three water molecules, and for DES III with four water molecules as inferred by a gradual increase in the intensity of Ha peak.

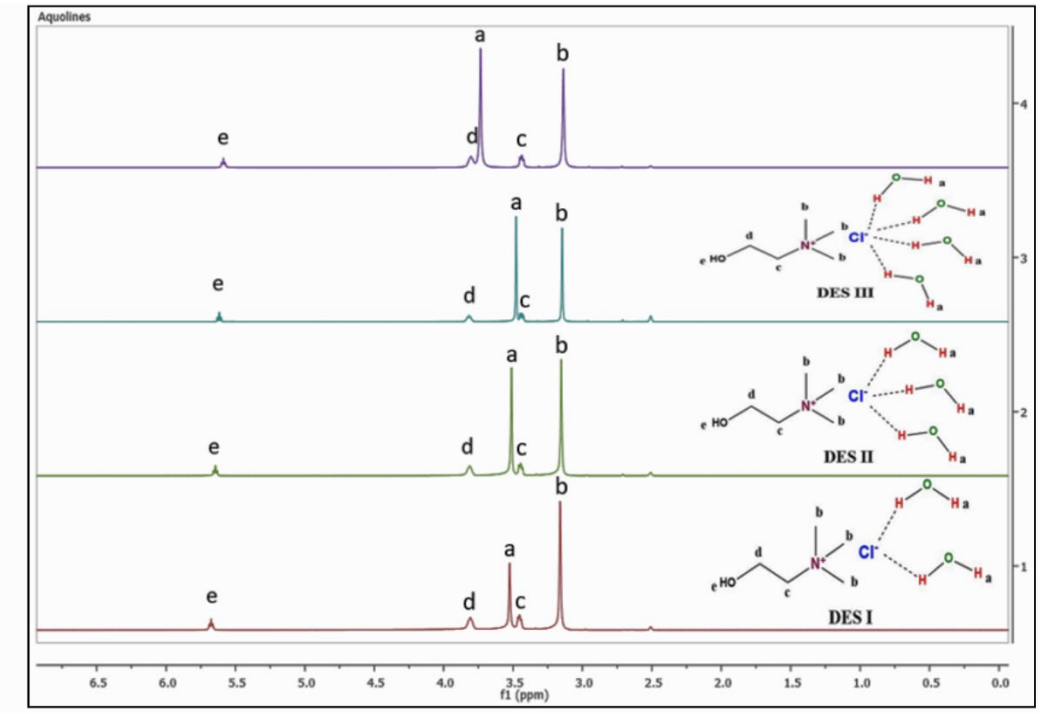

Figure 3.4: ^{1}H-NMR spectra of aquolines.

Contrary to this, chemical shift changes (for Ha and Hc) on moving from DES I to DES III reflect a change in internal interaction due to additional water molecules. However, DES IV shows different changes in chemical shift which may be due to less or absence of H-bonding. Further, by combining FTIR and ^{1}H NMR data for DES IV, one can draw the inference that the state of water in the DES skeleton has now changed and reflected spectroscopically.

c) Characterization of type-V DESs (hydrophobic DESs; HDES)

Figures 3.5 (a-b) show typical FTIR spectra for HDES. The composition of the reactants can affect the development of various interactions between molecules in mixtures [47]. Hydrogen bonds between two compounds, HBD and HBA lead to the development of eutectic mixtures. The sensitivity of FTIR to microstructural changes makes it ideal for studying hydrogen bonds. FTIR was used to identify the key functional groups and detect the creation of hydrogen bonds between components of DESs. **Figure 3.5 (a)** represents the FTIR spectra of TM-based DESs

at different eutectic compositions. The spectra of all TM-based DESs seem similar because they include the same HBA group, which was derived from menthol during the synthesis process. The menthol exhibited absorption bands at 3257 cm^{-1} due to -OH stretching. The FTIR spectra of LTTMs exhibited a prominent peak at 2959–2865 cm^{-1} attributed to the stretching of the -CH_3 group. The peaks at 1024 cm^{-1} correspond to the C=O bond, while the peak at 1375 cm^{-1} can be attributed to the stretching vibration of the isopropyl group. The FTIR spectra of all HDESs displayed an absorption peak at 1620 cm^{-1} attributed to the C-C stretching of the benzene ring of thymol. All functional groups in both components were detected, and the OH stretching band changed to a higher bandwidth in the spectra, confirming the development of HDESs.

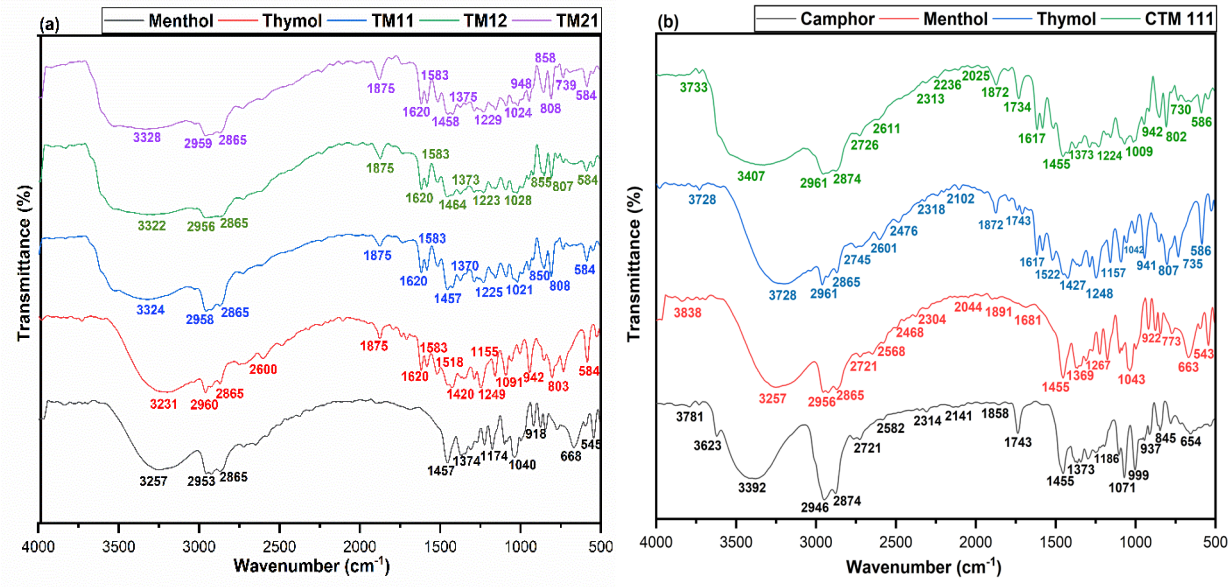

Figures 3.5: FTIR spectra of a) TM-based HDESs; b) CTM111.

The FTIR spectroscopy of thymol, menthol, camphor, and CTM111 is represented in **Figure 3.5 (b)**. In CTM111, the bandwidth is shifted towards a higher wavelength as compared to their starting components. The peak at 3623 cm^{-1} is attributed to the formation of hydrogen bonding among the camphor, menthol, and thymol. The prominent peak at 2959–2865 cm^{-1} is attributed to the stretching of the -CH_3 group which is shifted to 2946-2874 cm^{-1} in CTM111.

Figures 3.6 show typical ^{1}H NMR spectra for HDES. NMR spectroscopy was used to analyze the structure of molecules of the synthesized HDES. This will improve understanding of the connection between menthol, thymol, and camphor. The different chemical shifts experienced by the majority of protons in HDESs, including the paired OH groups of thymol and menthol exhibit the most significant shift as shown in **Figure 3.6**. As expected, the higher

thymol content results in a more pronounced chemical change of the OH–protons. When thymol is added slowly to menthol, their chemical shifts change in opposite directions compared to the pure molecules. The increase in the standard enthalpy changes of formation of thymol when menthol is present suggests that thymol protons are in a less shielded environment, making them more acidic as the amount of menthol increases. Conversely, the acidity of menthol decreases as the amount of thymol increases.

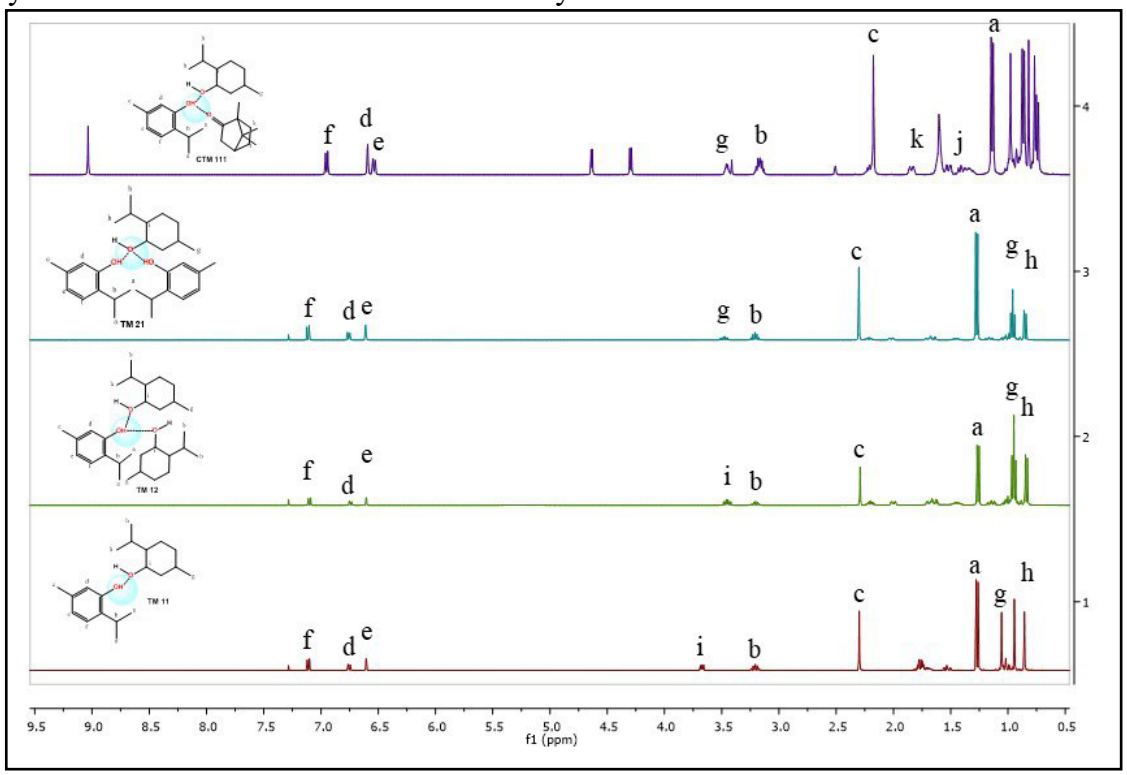

Figure 3.6: ^{1}H-NMR spectra of HDESs.

The signals for different interactions for TM11 are shown as: ^{1}H NMR (400 MHz, CDCl3) δ 7.11 (d, J = 7.8 Hz, 1H), 6.76 (dd, J = 7.8, 0.5 Hz, 1H), 6.61 (d, J = 0.8 Hz, 1H), 3.48 (td, J = 10.5, 4.3 Hz, 1H), 3.27 – 3.15 (m, 2H), 2.30 (s, 3H), 2.27 – 2.14 (m, 2H), 1.27 (d, J = 6.9 Hz, 6H), 0.96 (t, J = 6.9 Hz, 3H), 0.85 (d, J = 7.0 Hz, 6H); TM12 : ^{1}H NMR (400 MHz, CDCl3) δ 7.11 (d, J = 7.8 Hz, 1H), 6.76 (dd, J = 7.8, 0.5 Hz, 1H), 6.61 (d, J = 0.8 Hz, 1H), 3.48 (td, J = 10.5, 4.3 Hz, 2H), 3.27 – 3.15 (m, 2H), 2.30 (s, 3H), 2.27 – 2.14 (m, 2H), 1.27 (d, J = 6.9 Hz, 6H), 0.96 (t, J = 6.9 Hz, 6H), 0.85 (d, J = 7.0 Hz, 12H); TM21 : ^{1}H NMR (400 MHz, CDCl3) δ 7.11 (d, J = 7.8 Hz, 1H), 6.76 (dd, J = 7.8, 0.5 Hz, 1H), 6.61 (d, J = 0.8 Hz, 1H), 3.48 (td, J = 10.5, 4.3 Hz, 1H), 3.27 – 3.15 (m, 2H), 2.30 (s, 3H), 2.27 – 2.14 (m, 2H), 1.27 (d, J = 6.9 Hz, 12H), 0.96 (t, J = 6.9 Hz, 3H), 0.85 (d, J = 7.0 Hz, 6H); and CTM111: ^{1}H NMR (400 MHz, DMSO) δ 9.04 (s, 1H), 6.95 (d, J = 7.7 Hz, 1H), 6.71 – 6.31 (m, 2H), 4.64 (d, J = 4.1 Hz,

1H), 4.30 (d, J = 5.6 Hz, 1H), 3.44 (dd, J = 11.3, 7.1 Hz, 3H), 3.35 – 3.12 (m, 2H), 2.30 – 1.98 (m, 3H), 1.78 – 1.43 (m, 6H).

d) Characterization of ternary DESs (CUG I and CUG II)

The FTIR spectra of ChCl, urea, glycerol, and ternary DESs (CUG I and CUG II) show characteristic peaks representing various functional groups. **Figure 3.7** shows typical FTIR spectra for ternary DESs. ChCl exhibits peaks at 3259 cm^{-1} for O–H stretching, 2906 cm^{-1} for C–H stretching, 1477 cm^{-1} for C-N stretching, and 1136 cm^{-1} for C-O stretching. Urea exhibits peaks at 3442 cm^{-1} and 3343 cm^{-1} for asymmetrical and symmetrical stretching of N–H, 1684 cm^{-1} and 1615 cm^{-1} for C = O stretching, and 1464 cm^{-1} for C-N stretching. Glycerol exhibits peaks at 3570 cm^{-1} for O–H stretching, 1446 cm^{-1} for C-OH bending, and 1115 cm^{-1} for C-O stretching of primary alcohol. In the spectrum of CUG I and CUG II, shifts are observed. The OH stretching of ChCl shifts to 3614 cm^{-1} for CUG I and 3476 cm^{-1} for CUG II. These shifts are indicative of interactions (hydrogen bonding) between the components in the TDES structure.

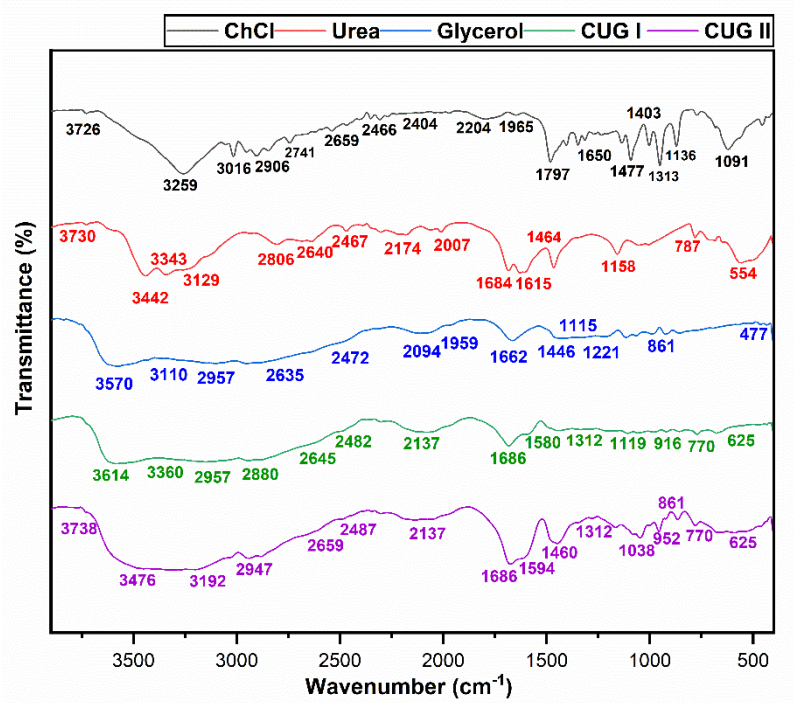

Figure 3.7: FTIR spectra of ternary DESs (CUG I and CUG II).

Figure 3.8 represents ^{1}H NMR spectra for CUG I and CUG II. The signals for different interactions are shown for CUG I as: ^{1}H NMR (400 MHz, DMSO) δ 5.51 (s, 4H), 4.64 – 4.39 (m, 2H), 3.83 (s,2H), 3.46 – 3.23 (m, 11H), 3.13 (s, 9H); and for CUG II as: ^{1}H NMR (400 MHz, DMSO) δ 5.58 (s, 8H), 4.67 – 4.50 (m, 2H), 3.82 (s, 2H), 3.42 (ddd, J = 15.7, 11.0, 6.6 Hz, 4H), 3.39 – 3.22 (m, 3H), 3.14 (s, 9H).

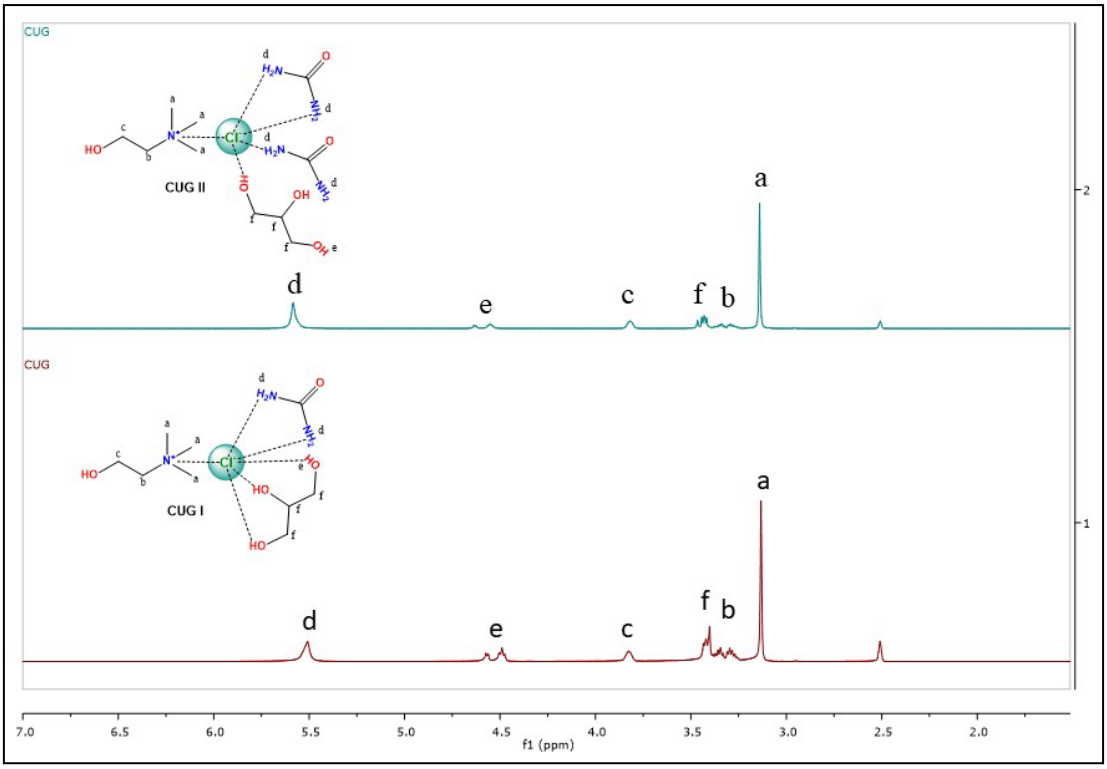

Figure 3.8: ^{1}H-NMR spectra of TDESs.

3.3.2 Physical properties of prepared DESs and DES-water mixture

Various physical properties of DESs and DESs-water mixtures are compiled in Table 3.1, Table 3.2, and Table 3.3.

3.3.2.1 Physical properties of water-based DESs (aquolines)

Table 3.1 compiles various physicochemical properties/parameters such as relative viscosities (η_r), zero shear viscosities (η_0), surface tensions (γ), contact angle (θ), specific conductance (κ), pH, densities (ρ), average composition molecular weight (M_{ac}), molar volume (V_m), calculated Gordon parameters (G), micro polarity (I_1/I_3) and apparent dielectric constant (ε, experienced by the probe in pure aquoline medium). The related data for water have also been provided for comparison purposes. M_{ac}, V_m, and G were obtained by the method reported in the literature [48–50]. Shear viscosity (η_s) has been measured for aquoline having different molar ratios of water (ChCl: H_2O: 1:2 (DES I), 1:3 (DES II), 1:4 (DES III), and 1:5 (DES IV)) at various shear rates (s^{-1}) (**Figure 3.9**). Data show that all aquoline samples behave as a Newtonian liquid. However, samples show Newtonian behaviour after certain stress. shear viscosity data are used to compute zero shear viscosities (η_0) which are compiled in **Table 3.1**.

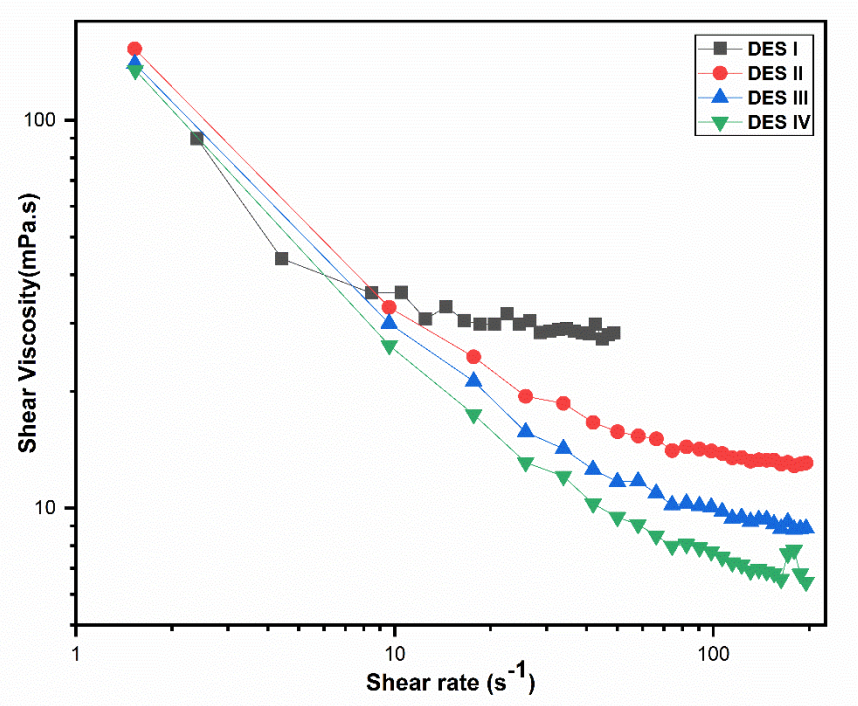

Figure 3.9: Variation of shear viscosity (η_s) against shear rate for aquolines.

η_0 decreases as the molar ratio of water to ChCl increases in typical aquoline samples. This may be due to variations in interactions (Ch-Ch, Ch-H_2O, Cl- H_2O, and H_2O - H_2O, etc.) between aquoline components. However, η_0 shows weak dependence (ranging from 176 to 155 for the molar ratio of H_2O from 2 -5) on the molar ratio of water to ChCl. The rheology experiment was also performed for aquoline with surfactant and salt. **Figure 3.10 (a-c)** shows the variation of shear stress vs. shear rate for various pure DESs or DES I + K-salt or DES I + K-salt + DTAB at 303±0.1 K. The data shows a linear variation of shear stress with shear rate indicating the Newtonian behaviour of all the DESs and this behaviour persists even with salt (KCl, KBr, or KNO_3) with or without surfactant. This Newtonian behaviour is similar to various conventional solvents like water, ethanol, glycerol, and dilute surfactant solutions [51,52]. Other DES-salt combinations (data not shown) show a similar nature of the resulting medium.

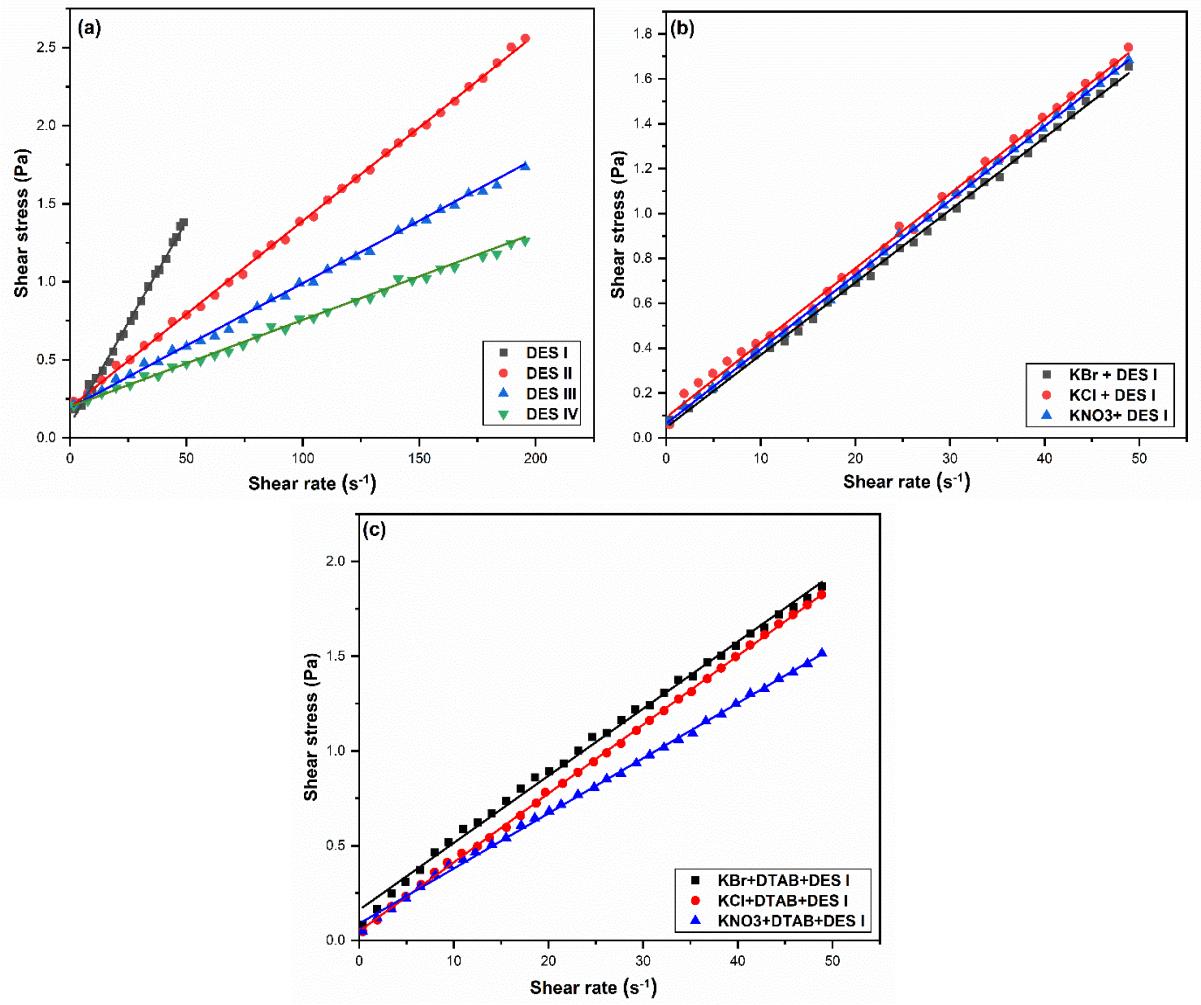

Figure 3.10: Variation of shear stress vs. shear rate for a) aquolines; b) K-salt + DES I; c) DTAB + K-salt + DES I at 303 ± 0.1K.

Contact angle data **(Figure 3.11 and Table 3.1)** for various *aquolines* (DES I to DES IV) have been compared with water to get information about the wettability of *aquolines*. DES I to DES III show a higher contact angle (though less than 90^0) than water, indicating they are less wettable than pure water. However, DES IV shows a contact angle nearly the same as water reflecting that the wettability pattern changes for this sample and meets the wetting property of water. This observation dictates that DES IV shows similar solvent properties to water and corroborates FTIR data (**Figure 3.3**) in which this sample of *aquoline* was a molecular solution of choline chloride in water and responsible for a similar contact angle of water and DES IV. Therefore, DES IV has not been used for further studies.

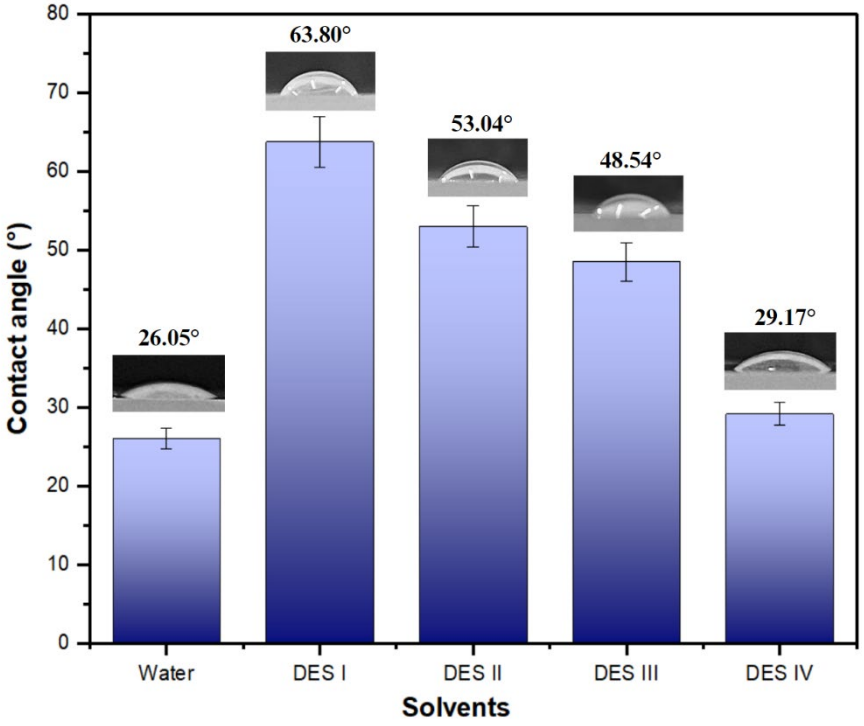

Figure 3.11: Contact angles of water and *aquolines* (DES I to DES IV).

pH values indicate that no significant change is observed with a varying molar ratio of water in aquoline (6.9-7.1). Therefore, such DES can be used in applications where acidity is an undesirable factor and shows superiority over hydrophobic DES (which shows an undesirable acidic nature) [53]. Moreover, κ increases with an increase in the molar ratio of water in a typical aquoline sample as observed with other DES systems [53–55]. This may be due to the weakening of electrostatic interaction and the contribution of individual ions of aquoline components. The micropolarity of aquoline system gradually decreases with a molar ratio of water in the sample. Further, micro polarity values are similar to those reported for other DES systems based on urea, glycerol, malonic acid, and ethylene glycol as hydrogen bond donors (HBD) to ChCl (hydrogen bond acceptor, HBA) [56,57]. However, polarity seems toward the higher side and matches nearly with reline.

A perusal of physical data for various *aquolines* suggests that they have both similarities and differences with pure water. G values have been found in the range (though lower) reported for pure water and can be used for the association investigation of a typical surfactant (DTAB, in the present case). The low G value may be due to different values of V_m associated with *aquolines*. However, the G value suggests that enough H-bonding interactions are present in a typical *aquoline*.

Table 3.1: Compilation of various physical properties of aquolines at 303±0.1 K.

Solvent	Relative viscosity (η_r)	Zero shear viscosity (η_0) (mPa.s)	Surface tension (γ) (mN. cm^{-1})	Contact angle (θ) (°)	Specific conductance (κ) (mS cm^{-1})	pH	Density (ρ) ($g.cm^{-4}$)	Average molar mass (M_{ac}) ($g.mol^{-1}$)	Molar volume (M_v) ($cm^3.mol^{-1}$)	Gordon parameter (G) ($J.m^{-3}$)	Micro polarity (I_1/I_3)	Apparent dielectric constant (ε)
DES I	28.5	176.64	62	63.8	18.3	6.93	1.097	58.54	53.36	1.65	2.52	120.74
DES II	14.57	175.5	70	53.04	42.2	6.9	1.091	48.4	44.37	1.98	2.49	118.69
DES III	7.93	160.83	66	48.54	55.9	6.98	1.078	42.32	39.26	1.94	2.47	116.68
DES IV	5.65	155.29	67	29.17	69.2	7.08	1.069	38.27	35.8	2	2.45	115.1
Water[a]	-	-	71.99	26.05	-	-	0.997	18.02	18	2.74	1.96	76.54

3.3.2.2 Physical properties of type-V DESs (hydrophobic DESs; HDES)

All the physical properties of HDESs are given in **Table 3.2**. The zero-shear viscosity (η_s) of all HDESs has been determined at different shear rates (s^{-1}) within the temperature range of 303K-323K. The rheology data for HDES samples, namely the viscosity as a function of shear rate and the shear stress as a function of shear rate, are presented in **Figure 3.12 (a-c)** for different temperatures. Data indicates that all samples exhibit the characteristics of Newtonian fluids.

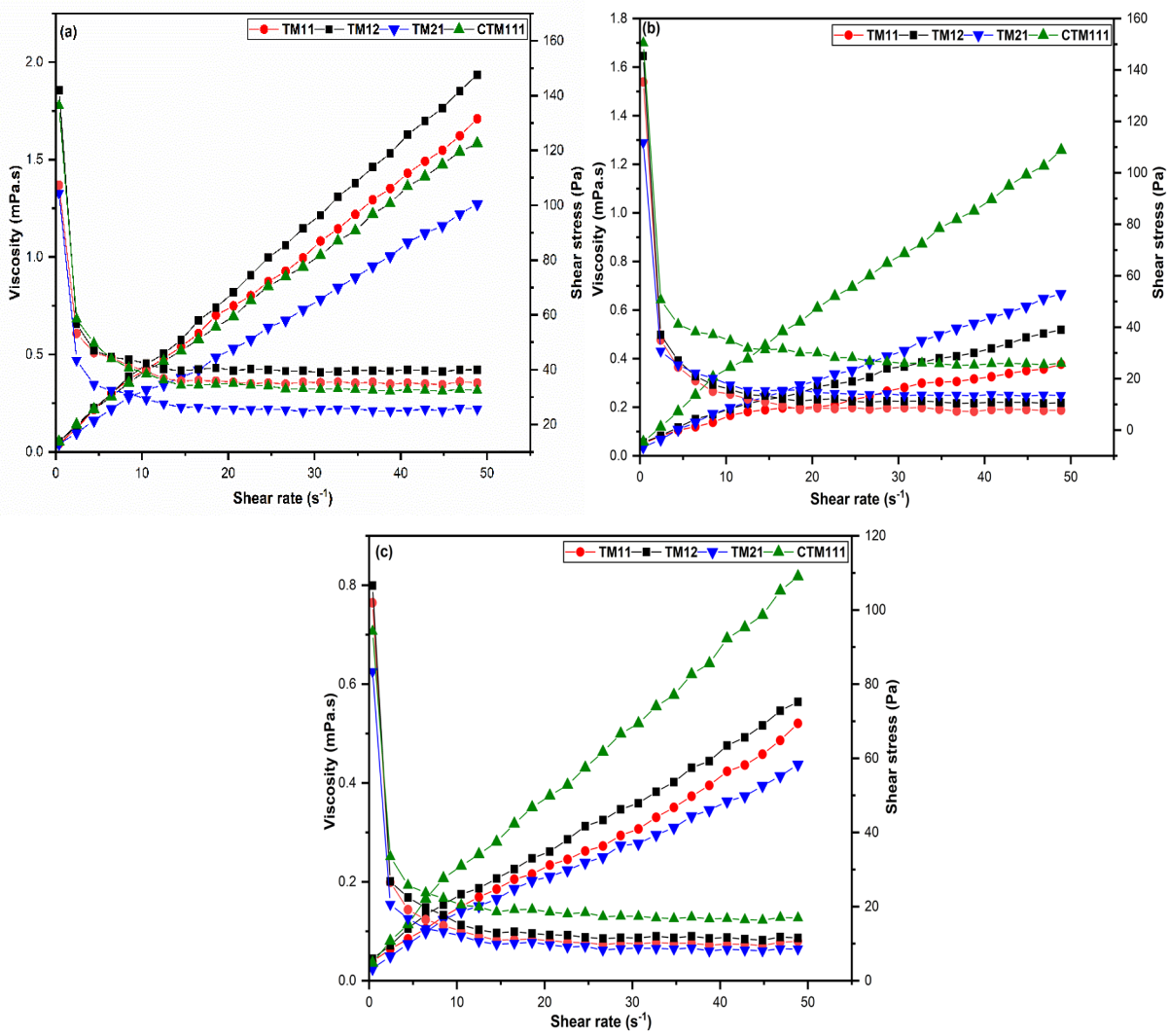

Figure 3.12: Newtonian behaviour in measured viscosity (left axis) and stress (right axis) as a function of shear rate for the HDESs at: a) 303 K; b) 313 K; and c) 323 K.

It is observed that pH and density values decrease with increases in temperature as observed for pure water. It was noted that maintaining a constant content of thymol and increasing the concentration of menthol resulted in an increase in the pH of the HDES. The

conductance of HDESs was found almost equal for all compositions, showing that HDESs are non-conducting.

Table 3.2: Compilation of physical properties of HDESs.

Systems	Zero shear viscosity (mPa.s)			pH			Density (g.cm^{-3})			Relative viscosity (η_r)	Conductance (µS)
	303 K	313 K	323 K	303 K	313 K	323 K	303 K	313 K	323 K	303 K	303 K
TM11	154.31	117.60	116.18	6.05	6.01	5.93	0.925	0.919	0.912	29.39	0.83
TM12	165.89	158.16	121.68	6.40	6.28	6.16	0.915	0.908	0.905	34.51	0.84
TM21	127.13	116	95.29	7.20	7.08	6.90	0.940	0.930	0.927	22.06	0.84
CTM111	169.48	151	105.76	6.46	6.38	6.24	0.937	0.928	0.925	56.68	0.82

3.3.2.3 Physical properties of reline-water mixture

All the physicochemical properties of the reline-water mixture are compiled in **Table 3.3.** Zero shear viscosity (η_s) has been measured for pure reline, water in reline, and reline in water (10-90%) at various shear rates (s^{-1}) at 303K-323K. Rheology data (η_s *vs.* shear rate and stress *vs.* shear rate) of some of reline-water samples are shown in **Figure 3.13**. Data show that all samples behave as Newtonian fluids as observed for reline and other DES in earlier studies [58,59]. η_0 values were obtained from η_s *vs* shear rate and plotted (**Figure 3.14**) against the weight % of water in the mixture (water in reline to reline in water).

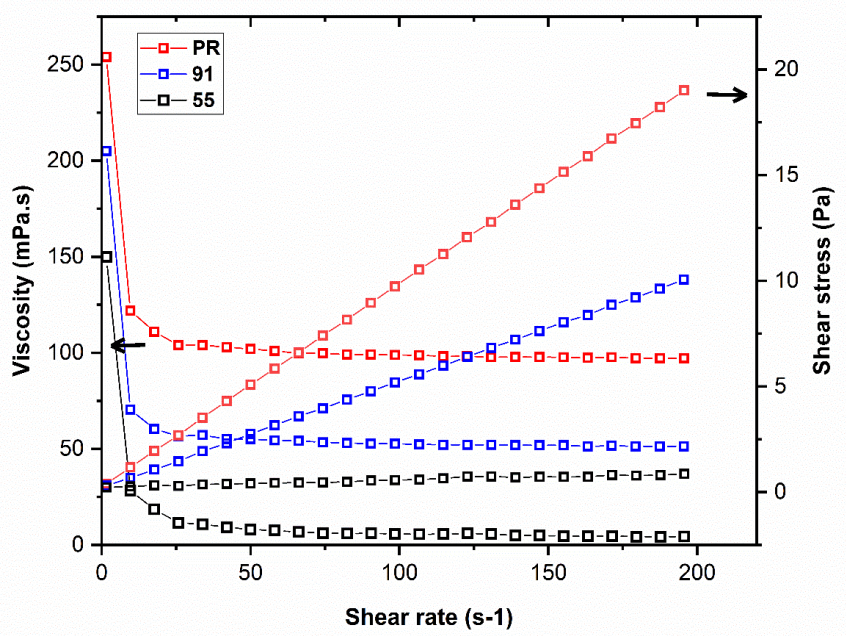

Figure 3.13: Newtonian behaviour in measured viscosity (left axis) and stress (right axis) as a function of shear rate for the reline + water mixture: □ pure reline; □ 10% water and □ 55%water.

Figure 3.14 shows three regions in which viscosity decreases sharply (region 1) and then shows an increase (region 2) followed by a gradual decrease (region 3). It seems that water in reline converts into reline in water in region 2, which may be due to the conversion of DES to molecular component(s) solution. η_0 has been found 279 mPa.s (at 308K) and 453 mPa.s (at 303K) for pure reline. However, the reported value of η_0 for pure reline is 632 mPa.s (at 298K) [57]. This difference in η_0 values may be due to temperature differences (higher in the present study). It was noticed that an increase in temperature is responsible for the decrease in η_0 [49,60]. Therefore, our η_0 values are in order **(Table 3.3)** as reported in the literature [2, 7]. The relative viscosity (η_r) of reline-water mixture is also given in **Table 3.3**. It was observed that η_r increases with a decrease in water content and decreases with temperature increases.

Specific conductance (κ) data show an increase with an increase of water content and in accordance (~ 6%) with reported data for pure reline [57].

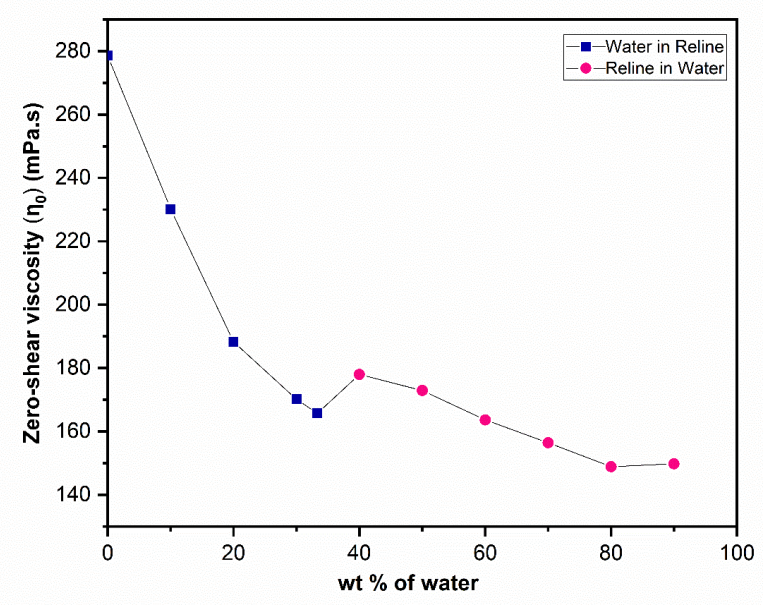

Figure 3.14: Variation of zero shear viscosity (η_0) against wt.% of water at 303 K.

The nature of type-III DESs has recently been distinguished in terms of their hydrophobicity/hydrophilicity or acidic /basic [53,61]. It has been known that a small addition of water (or increasing the temperature), to a typical DES, causes substantial changes in the physical properties of the anhydrous form [62–65]. **Table 3.3** also shows the variation of pH with mole fraction of water at different temperatures (303K-323K). pH of pure reline decreases with added water as well as by increasing temperature. The reline pH is matches with the reported value in the literature and validates the study [61]. Simulation studies have shown that a small amount of water disturbs H-bonding among Cl ions (of ChCl) and the urea molecules due to the strong solvation of Cl^- by the action of water as a second HBD [66]. Since water renders an acidic aqueous subphase with a [67–69] high halide ion concentration which may reduce the overall pH of the reline-water mixture [53]. However, heating may cause an increase in the kinetic energy of DES network responsible for the depletion of intermolecular hydrogen bonding with a concomitant shifting of the chemical equilibrium towards dissociation of more H^+ ions with an overall pH decrease with an increase in temperature [70].

Table 3.3: Compilation of physical properties of reline-water mixture in water in reline and reline in water region.

Properties / Systems / Temp / Wt.% of water	Zero shear viscosity (mPa.s)			pH			Density (g.cm^{-3})			Molar Volume (m^3.mol^{-1})		
	303 K	313 K	323 K	303 K	313 K	323 K	303 K	313 K	323 K	303 K	313 K	323 K
Water 100	-	-	-	7.02	6.9	6.85	0.995	0.992	0.988	18.073	18.14	18.21
RW19 90	149.77	124.48	165.23	9.09	8.94	8.83	1.016	1.014	1.010	41.50	41.57	41.72
RW28 80	148.86	156.63	160.67	9.32	9.10	8.94	1.039	1.033	1.030	63.83	64.17	64.39
RW37 70	156.45	165.53	151.50	9.41	9.20	9.03	1.060	1.054	1.050	85.36	85.80	86.16
RW46 60	163.64	133.61	142.07	9.48	9.27	9.10	1.080	1.075	1.070	106.16	106.67	107.11
RW55 50	172.94	144.76	185.50	9.55	9.35	9.18	1.099	1.093	1.089	126.25	126.98	127.46
RW64 40	177.98	142.35	153.97	9.67	9.47	9.31	1.118	1.112	1.108	145.76	146.50	147.11
RW6633 33.3	165.72	211.66	144.16	9.79	9.57	9.41	1.132	1.126	1.122	156.68	157.42	157.96
RW73 30	170.17	129.65	167.93	9.86	9.64	9.50	1.138	1.132	1.127	164.44	165.33	166.11
RW82 20	188.27	170.98	216.01	10.06	9.85	9.71	1.158	1.157	1.147	182.50	183.52	184.20
RW91 10	230.14	178.18	183.42	10.33	10.12	10.00	1.175	1.168	1.165	200.38	201.53	202.15
Reline 0	453	229.71	188.95	10.38	10.20	10.04	1.190	1.184	1.180	218.87	219.36	220.04

Properties / Systems	Temp / Wt.% of water	Relative viscosity (η_r) (mPa.s)			Refractive index			Surface tension (dyne.cm^{-1})	Specific conductance mS.cm^{-1}	Micro polarity (I_1/I_3)
		303 K	313 K	323 K	303 K	313 K	323 K	303 K	303 K	303 K
Water	100	-	-	-	1.336	1.335	1.334	67	-	1.65
RW19	90	1.176	1.162	1.156	1.352	1.351	1.350	50	-	1.84
RW28	80	1.294	1.271	1.267	1.370	1.368	1.367	49	-	1.95
RW37	70	1.431	1.400	1.389	1.387	1.386	1.384	48	-	2.05
RW46	60	1.754	1.735	1.725	1.407	1.402	1.401	54	-	2.10
RW55	50	2.225	2.203	2.186	1.421	1.419	1.417	56	-	2.20
RW64	40	2.823	2.796	2.764	1.437	1.435	1.434	61	56.5	2.28
RW6633	33.3	3.598	3.574	3.543	1.450	1.448	1.446	60	44.8	2.33
RW73	30	6.372	6.356	6.326	1.455	1.454	1.451	62	41.7	2.36
RW82	20	6.588	6.547	6.503	1.470	1.468	1.467	64	15.52	2.43
RW91	10	38.66	37.13	34.32	1.486	1.485	1.484	72	4.45	2.50
Reline	0	-	-	-	1.497	1.496	1.495	76	0.68	2.34

Densities (at 303K-323K) of pure reline, water, and its mixture with water (at different temperatures) are compiled in **Table 3.3**. Data show that the densities are in good agreement with the values reported in the literature [49,71] and further validate the purity and procedure. Contrasting trends of density decrease with temperature have been reported in the last decades [49,67–69,72]. Density values are used to determine molar volumes of binary mixtures using the following well-known equation

$$M_{mix} = \frac{X_1 m_1 + X_2 m_2}{\rho_{sol}} \quad \text{(Equation 1)}$$

Where, X_1=mole fraction of water

m_1= molecular weight of water

X_2=mole fraction of reline

m_2= molecular weight of reline

ρ_{sol} = density of solution

The value of surface tension for reline-water mixture shows an irregular trend may be due to complex structure of reline and the change in the structure of reline while adding water. The micro polarity of reline-water mixture gradually increases with a decrease in water content. However, the micro polarity of pure reline is in between the mixture with 33.3 % and 30 % water content. It may be due to the transition of DES to molecular solution. To determine the potential application of DESs in industrial and chemical processes, understanding their physical qualities such as refractive index is essential. These could also offer crucial insights into the purity of the samples and the molecular interactions in the liquid [73]. It is observed that the refractive index increases with a decrease in water content in reline-water mixture and decreases with an increase in temperature.

3.4 Conclusion

Various types of DESs were synthesized, including Type-III (reline, ethaline, glyceline), water-based DESs (aquolines), hydrophobic DESs (HDES), and ternary DESs (TDESs). The synthesis involved mixing specific components in precise molar ratios and subjecting them to controlled heating and stirring conditions. The DESs were characterized using Fourier Transform Infrared (FTIR) spectroscopy and Nuclear Magnetic Resonance (NMR) spectroscopy. FTIR spectra provided insights into the chemical interactions and bonding within the DESs. NMR spectra revealed structural information about the DES

components and their interactions. The characterization confirmed the formation of DESs and provided details about their molecular structure and composition. FTIR and ^{1}H NMR data show the transition of aquolines into a molecular solution of ChCl at a definite number of water molecules (1:5) in a typical ChCl-water system. Various physical properties of DESs were measured, including viscosity, surface tension, contact angle, specific conductance, pH, densities, molecular weight, molar volume, polarity, and dielectric constant. The rheology data shows that all DESs behave as Newtonian fluids. Different DESs exhibited distinct physical and chemical properties based on their composition and molecular interactions. Physicochemical data suggest that aquolines have some similarities (density, surface tension, or Newtonian behaviour) with water and some differences in other physical properties (relative viscosity or Gordon parameter). Aquoline has been found Newtonian, nearly neutral (pH ~7), electrically conducting, and highly polar fluids. pH, density, and viscosity values decrease with an increase in temperature. The study provided valuable data for understanding the behavior of DESs in various applications, such as solvent systems, electrolytes, and reaction media. The characterization and physical property measurements contribute to the ongoing research and development of DESs for diverse industrial and scientific purposes.

3.5 References

[1] E. L. Smith, A. P. Abbott, and K. S. Ryder, Chemical Reviews.

[2] S. K. Singh and A. W. Savoy, J Mol Liq **297**, 112038 (2020).

[3] B. B. Hansen, S. Spittle, B. Chen, D. Poe, Y. Zhang, J. M. Klein, A. Horton, L. Adhikari, T. Zelovich, B. W. Doherty, B. Gurkan, E. J. Maginn, A. Ragauskas, M. Dadmun, T. A. Zawodzinski, G. A. Baker, M. E. Tuckerman, R. F. Savinell, and J. R. Sangoro, Chemical Reviews.

[4] A. P. Abbott, G. Capper, D. L. Davies, R. K. Rasheed, and V. Tambyrajah, Green Chemistry **4**, 24 (2002).

[5] M. Q. Farooq, N. M. Abbasi, and J. L. Anderson, J Chromatogr A **1633**, 461613 (2020).

[6] S. A. Forsyth, J. M. Pringle, and D. R. MacFarlane, Aust J Chem **57**, 113 (2004).

[7] R. E. Del Sesto, C. Corley, A. Robertson, and J. S. Wilkes, J Organomet Chem **690**, 2536 (2005).

[8] X. Yue, T. Suopajärvi, O. Mankinen, M. Mikola, A. Mikkelson, J. Ahola, S. Hiltunen, S. Komulainen, A. M. Kantola, V.-V. Telkki, and H. Liimatainen, J Agric Food Chem **68**, 15074 (2020).

[9] M. Reynolds, L. M. Duarte, W. K. T. Coltro, M. F. Silva, F. J. V. Gomez, and C. D. Garcia, Microchemical Journal **157**, 105067 (2020).

[10] A. P. R. Santana, J. A. Mora-Vargas, T. G. S. Guimarães, C. D. B. Amaral, A. Oliveira, and M. H. Gonzalez, J Mol Liq **293**, 111452 (2019).

[11] D. E. Crawford, L. A. Wright, S. L. James, and A. P. Abbott, Chemical Communications **52**, 4215 (2016).

[12] T. Loftsson and M. E. Brewster, Journal of Pharmacy and Pharmacology **62**, 1607 (2010).

[13] L. Zamora, C. Benito, A. Gutiérrez, R. Alcalde, N. Alomari, A. Al Bodour, M. Atilhan, and S. Aparicio, Physical Chemistry Chemical Physics **24**, 512 (2022).

[14] C. Florindo, M. M. Oliveira, L. C. Branco, and I. M. Marrucho, J Mol Liq **247**, 441 (2017).

[15] M. Ivanović, M. Islamčević Razboršek, and M. Kolar, Plants **9**, 1428 (2020).

[16] P. A. Shah, V. Chavda, D. Hirpara, V. S. Sharma, P. S. Shrivastav, and S. Kumar, J Mol Liq **390**, 123171 (2023).

[17] Q. Zhang, K. De Oliveira Vigier, S. Royer, and F. Jérôme, Chem Soc Rev **41**, 7108 (2012).

[18] G. García, S. Aparicio, R. Ullah, and M. Atilhan, Energy & Fuels **29**, 2616 (2015).

[19] Y. Liu, J. B. Friesen, J. B. McAlpine, D. C. Lankin, S.-N. Chen, and G. F. Pauli, J Nat Prod **81**, 679 (2018).

[20] K. A. Omar and R. Sadeghi, J Mol Liq **360**, 119524 (2022).

[21] C. Chiappe and D. Pieraccini, J Phys Org Chem **18**, 275 (2005).

[22] D. A. Alonso, A. Baeza, R. Chinchilla, G. Guillena, I. M. Pastor, and D. J. Ramón, European J Org Chem **2016**, 612 (2016).

[23] Md. S. Alam and A. M. Siddiq, J Mol Liq **242**, 1075 (2017).

[24] V. Agieienko and R. Buchner, J Chem Eng Data **65**, 1900 (2020).

[25] C. W. Extrand, Colloids Surf A Physicochem Eng Asp **679**, 132545 (2023).

[26] A. Ghoufi, P. Malfreyt, and D. J. Tildesley, Chem Soc Rev **45**, 1387 (2016).

[27] A. Akram, G. Shaw, R. J. Lewis, M. Piccinini, D. J. Morgan, T. E. Davies, S. J. Freakley, J. K. Edwards, J. A. Moulijn, and G. J. Hutchings, Catal Sci Technol **10**, 8203 (2020).

[28] C. Chalbaud, M. Robin, J.-M. Lombard, F. Martin, P. Egermann, and H. Bertin, Adv Water Resour **32**, 98 (2009).

[29] M. H. Zainal-Abidin, M. Hayyan, G. C. Ngoh, and W. F. Wong, ACS Omega **5**, 1656 (2020).

[30] W. Li, W. Kong, W. Liu, S. Xu, H. Zhu, S. Liu, W. Yu, and Z. Wen, Energy Storage Mater **65**, 103103 (2024).

[31] L. Meneses, F. Santos, A. R. Gameiro, A. Paiva, and A. R. C. Duarte, Journal of Visualized Experiments (2019).

[32] T. Zhekenov, N. Toksanbayev, Z. Kazakbayeva, D. Shah, and F. S. Mjalli, Fluid Phase Equilib **441**, 43 (2017).

[33] M. S. Rahman and D. E. Raynie, J Mol Liq **324**, 114779 (2021).

[34] D. Hirpara, B. Patel, V. Chavda, A. Desai, and S. Kumar, J Mol Liq **364**, 119991 (2022).

[35] D. Lapeña, F. Bergua, L. Lomba, B. Giner, and C. Lafuente, J Mol Liq **303**, 112679 (2020).

[36] R. Haghbakhsh and S. Raeissi, J Chem Thermodyn **147**, 106124 (2020).

[37] M. Sajjadur Rahman, J. Kyeremateng, M. Saha, S. Asare, N. Uddin, M. A. Halim, and D. E. Raynie, J Mol Liq **350**, 118520 (2022).

[38] T. Raja Sekharan, R. Margret Chandira, S.C. Rajesh, Shunmugaperumal Tamilvanan, CT. Vijayakumar, and B.S. Venkateswarlu, Biointerface Res Appl Chem **11**, 14620 (2021).

[39] G. Almustafa, R. Sulaiman, M. Kumar, I. Adeyemi, H. A. Arafat, and I. AlNashef, Chemical Engineering Journal **395**, 125173 (2020).

[40] M. A. Kadhom, G. H. Abdullah, and N. Al-Bayati, Arab J Sci Eng **42**, 1579 (2017).

[41] R. S. Atri, A. Sanchez-Fernandez, O. S. Hammond, I. Manasi, J. Doutch, J. P. Tellam, and K. J. Edler, Journal of Physical Chemistry B **124**, 6004 (2020).

[42] C. Du, B. Zhao, X.-B. Chen, N. Birbilis, and H. Yang, Sci Rep **6**, 29225 (2016).

[43] M. Nedaei, A. R. Zarei, and S. A. Ghorbanian, New Journal of Chemistry **42**, 12520 (2018).

[44] Y. M. AlZahrani and M. M. Britton, Physical Chemistry Chemical Physics **23**, 21913 (2021).

[45] R. K. Banjare, M. K. Banjare, K. Behera, S. Pandey, and K. K. Ghosh, ACS Omega **5**, 19350 (2020).

[46] H. Dong, Z. Zhang, Z. Qiu, D. Tang, and J. Shu, J Phys Chem B **127**, 1013 (2023).

[47] B. D. Ribeiro, C. Florindo, L. C. Iff, M. A. Z. Coelho, and I. M. Marrucho, ACS Sustain Chem Eng **3**, 2469 (2015).

[48] Komal, G. Singh, G. Singh, and T. S. Kang, ACS Omega **3**, 13387 (2018).

[49] V. Agieienko and R. Buchner, J Chem Eng Data **64**, 4763 (2019).

[50] R. S. Atri, A. Sanchez-Fernandez, O. S. Hammond, I. Manasi, J. Doutch, J. P. Tellam, and K. J. Edler, J Phys Chem B **124**, 6004 (2020).

[51] S. S. Pawar and V. K. Sunnapwar, Exp Therm Fluid Sci **44**, 792 (2013).

[52] H. Rehage and H. Hoffmann, Mol Phys **74**, 933 (1991).

[53] H. Kivelä, M. Salomäki, P. Vainikka, E. Mäkilä, F. Poletti, S. Ruggeri, F. Terzi, and J. Lukkari, Journal of Physical Chemistry B **126**, 513 (2022).

[54] W. Guo, Y. Hou, S. Ren, S. Tian, and W. Wu, J Chem Eng Data **58**, 866 (2013).

[55] C. Ma, A. Laaksonen, C. Liu, X. Lu, and X. Ji, Chemical Society Reviews.

[56] A. Pandey, R. Rai, M. Pal, and S. Pandey, Physical Chemistry Chemical Physics **16**, 1559 (2014).

[57] E. L. Smith, A. P. Abbott, and K. S. Ryder, Chemical Reviews.

[58] O. S. Hammond, D. T. Bowron, and K. J. Edler, ACS Sustain Chem Eng **7**, 4932 (2019).

[59] C. D'Agostino, L. F. Gladden, M. D. Mantle, A. P. Abbott, E. I. Ahmed, A. Y. M. Al-Murshedi, and R. C. Harris, Physical Chemistry Chemical Physics **17**, 15297 (2015).

[60] G. H. Abdullah and M. A. Kadhom, Studying of Two Choline Chloride's Deep Eutectic Solvents in Their Aqueous Mixtures, 2016.

[61] F. S. Mjalli and O. U. Ahmed, Korean Journal of Chemical Engineering **33**, 337 (2016).

[62] V. Agieienko and R. Buchner, J Chem Eng Data **64**, 4763 (2019).

[63] D. Shah and F. S. Mjalli, Physical Chemistry Chemical Physics **16**, 23900 (2014).

[64] S. Ruggeri, F. Poletti, C. Zanardi, L. Pigani, B. Zanfrognini, E. Corsi, N. Dossi, M. Salomäki, H. Kivelä, J. Lukkari, and F. Terzi, Electrochim Acta **295**, 124 (2019).

[65] C. H. J. T. Dietz, M. C. Kroon, M. van Sint Annaland, and F. Gallucci, J Chem Eng Data **62**, 3633 (2017).

[66] O. S. Hammond, D. T. Bowron, A. J. Jackson, T. Arnold, A. Sanchez-Fernandez, N. Tsapatsaris, V. Garcia Sakai, and K. J. Edler, Journal of Physical Chemistry B **121**, 7473 (2017).

[67] D. Z. Troter, Z. B. Todorović, D. R. Đokić-Stojanović, B. S. Đordević, V. M. Todorović, S. S. Konstantinović, and V. B. Veljković, Journal of the Serbian Chemical Society **82**, 1039 (2017).

[68] Y. Xie, H. Dong, S. Zhang, X. Lu, and X. Ji, J Chem Eng Data **59**, 3344 (2014).

[69] R. B. Leron and M. H. Li, Journal of Chemical Thermodynamics **54**, 293 (2012).

[70] F. S. Mjalli and O. U. Ahmed, Asia-Pacific Journal of Chemical Engineering **11**, 549 (2016).

[71] D. Lapeña, F. Bergua, L. Lomba, B. Giner, and C. Lafuente, J Mol Liq **303**, (2020).

[72] Y. Wang, C. Ma, C. Liu, X. Lu, X. Feng, and X. Ji, J Chem Eng Data **65**, 2446 (2020).

[73] R. B. Leron, A. N. Soriano, and M. H. Li, J Taiwan Inst Chem Eng **43**, 551 (2012).